Realization of Dual-Frequency and Wide-Band VSWR Performances Using Normal-Mode Helical and Inverted-F Antennas

Hisamatsu Nakano, *Fellow, IEEE*, Noriaki Ikeda, Yu-Yuan Wu, Ryota Suzuki, Hiroaki Mimaki, *Member, IEEE*, and Junji Yamauchi, *Member, IEEE*

***Abstract*— The effects of parasitic elements on the voltage standing wave ratios (VSWR's) of two antennas are investigated. First, a parasitic monopole is used for a normal-mode helical antenna. The VSWR investigation shows that dual-frequency operation is obtained by the parasitic element effects. The dual-frequency operation is revealed as a function of monopole position above a ground plane (monopole height). As the monopole height decreases, the separation of a higher resonance frequency f_H from a lower resonance frequency f_L increases. For a monopole length of $L_{MP} \approx 0.4\lambda_{\rm HX}$, where $\lambda_{\rm HX}$ is the resonance wavelength of the helix, the frequency bandwidth for a VSWR $= 2$ criterion is 12.5% in the lower frequency f_L region and 5.2% in the higher frequency f_H region, with a frequency separation ratio of $f_H/f_L = 2.14$. Secondly, L-figured parasitic elements are used for an inverted-F antenna (IFA). The parasitic elements improve the VSWR performance. The frequency bandwidth for a VSWR $= 2$ criterion is approximately two times as wide as that of the single IFA. It is also found that bending the horizontal sections of the IFA and parasitic elements contributes to reducing the antenna size while not significantly deteriorating the VSWR bandwidth. The radiation patterns are also presented and discussed.**

***Index Terms*—Antennas, multifrequency antennas.**

I. Introduction

NORMAL-MODE helical [1] and inverted-F antennas (IFA's) [2] have been used as antennas for a portable telephone, which are placed outside and inside the handset, respectively [3], [4]. Antennas for wireless communication systems, such as personal satellite communication and cellular network systems, are required to have a dual-frequency (frequencies for transmission and reception) performance or a wide-band voltage standing wave ratio (VSWR) performance. This paper presents techniques to realize the dual-frequency and wide-band VSWR performances using normal-mode helical and IFA's with parasitic elements.

The experimental work by the authors in 1992 [5]–[7] showed that a normal-mode helical antenna with a monopole has multiple resonance frequencies. In this antenna system, the monopole is not in contact with the helix, i.e., the monopole acts as a parasitic element. Recently, Erätuuli *et al.* investigated a similar antenna system [8], where a monopole is combined with a helix.

The first part of this paper is devoted to the theoretical investigations of an antenna system composed of a feed helix and a parasitic monopole [5]. Special attention is paid to the behavior of dual-frequency operation for the antenna system. The dual-frequency performance is evaluated from the VSWR relative to 50 Ω. The frequency ratios f_H/f_L are calculated as a function of the monopole height $z_{\rm MP}$ for various values of monopole length $L_{\rm MP}$, where f_H and f_L are higher and lower resonance frequencies of the antenna system, respectively. The radiation pattern is also presented and discussed together with the current distributions of the monopole and the helix.

The second part of this paper is devoted to realization of wide-band VSWR performance for a low-profile IFA [2], [4], [9]–[15]. It is known that when the IFA height from a conducting ground plane is approximately one-tenth of the wavelength, the frequency bandwidth for a VSWR $= 2$ criterion is approximately 8%. In this paper, two L-figured parasitic elements are added to the IFA to widen the VSWR bandwidth. It is revealed that the VSWR bandwidth for the IFA with the parasitic elements is approximately two times as wide as that of the single IFA (note that this kind of bandwidth enhancement using a parasitic element has been found for a plate-type IFA (or L antenna) by Virga and Rahmat-Samii [16]).

Bending the horizontal sections of the present IFA and parasitic elements contributes to reducing the antenna size. For this, the VSWR performance for the bent antenna configuration is investigated. It is found that the bent IFA with the bent parasitic elements does not significantly deteriorate the VSWR bandwidth.

The current distributions along the helix and IFA systems considered in this paper are analyzed using the method of moments [17], [18] (the Galerkin method in which the piecewise sinusoidal functions are used for both basis and testing functions). On the basis of the calculated current distributions, the antenna characteristics, including the input impedance, VSWR, radiation pattern, and gain, are evaluated. For confirmation of these calculated values, some measured data are presented.

II. Dual-Frequency Performance of a Normal-Mode Helix with a Parasitic Monopole

A. Configuration

Fig. 1 shows the configuration and coordinate system of a feed helix and a parasitic monopole (HX-MP). The HX-MP

Manuscript received February 28, 1997; revised December 29, 1997.

The authors are with the College of Engineering, Hosei University, Koganei, Tokyo 184, Japan.

Publisher Item Identifier S 0018-926X(98)04309-9.

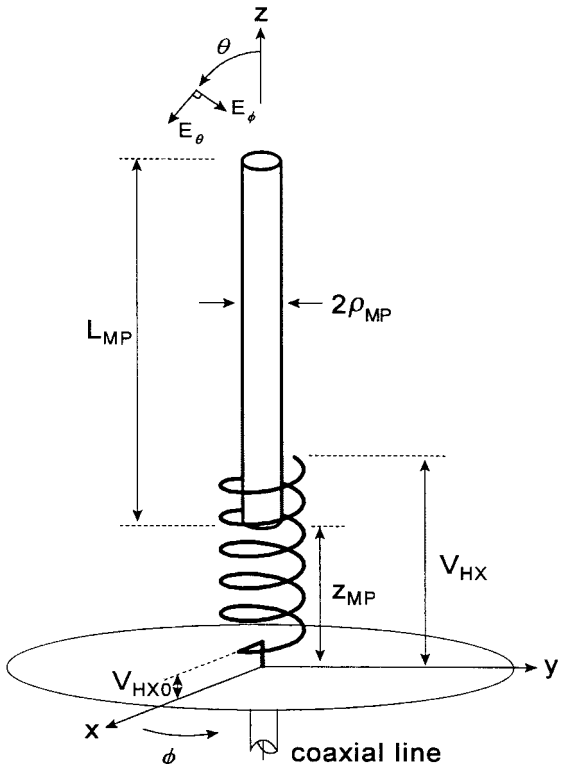

Fig. 1. An antenna system composed of a normal-mode helix and a monopole.

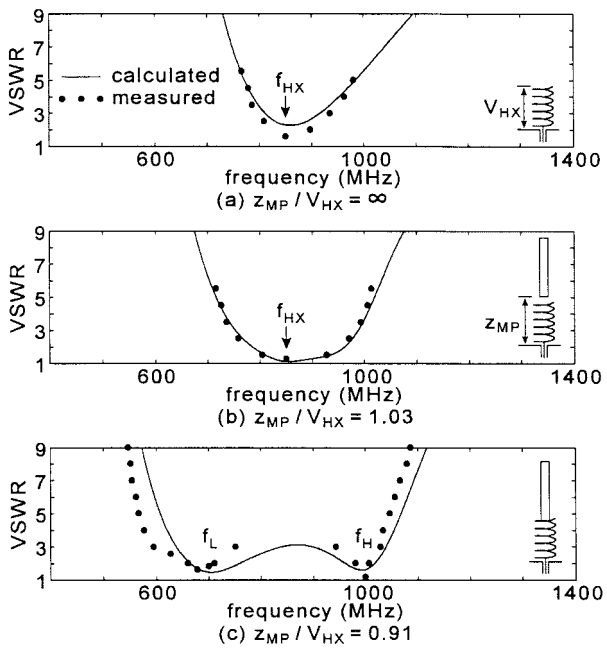

Fig. 2. VSWR as a function of relative monopole height $z_{\rm MP}/V_{\rm HX}$ $(= z_{\rm MP}/0.18\lambda_{\rm HX})$. The monopole length $L_{\rm MP}$ is kept constant: $L_{\rm MP} = 14$ cm $\approx 0.4\lambda_{\rm HX}$. (a) Helix without monopole $(z_{\rm MP}/V_{\rm HX} = \infty)$. (b) $z_{\rm MP}/V_{\rm HX} = 1.03$ (c) $z_{\rm MP}/V_{\rm HX} = 0.91$.

is located above a conducting ground plane of infinite extent. The monopole, made of a wire of radius $\rho_{\rm MP}$, has a length of $L_{\rm MP}$ and is located at $z = z_{\rm MP}$ (monopole height) on the z axis. The helix, made of a wire of radius $\rho_{\rm HX}$, is a normal-mode helix [1] specified by vertical length $V_{\rm HX}$, circumference C, pitch angle α, number of turns n, and height $V_{\rm HX0}$.

Throughout Section II, the parameters except for $z_{\rm MP}$ and $L_{\rm MP}$ are fixed: $\rho_{\rm MP} = 0.15$ cm, $\rho_{\rm HX} = 0.03$ cm, $V_{\rm HX} = 6.45$ cm, $C = 1.48$ cm, $\alpha = 37.5°$, $n = 5.625$ turns, and $V_{\rm HX0} = 0.075$ cm. The helix is fed from a 50-Ω coaxial line.

B. Effects of Antenna Height $z_{\rm MP}$ on Dual-Frequency Performance

Calculations show that the helix without the monopole resonates at $f = 850$ MHz $(\equiv f_{\rm HX})$ with a VSWR of 2.23. This is shown in Fig. 2(a). The vertical length of the helix is $V_{\rm HX} = 0.18\lambda_{\rm HX}$ at the resonance, where $\lambda_{\rm HX}$ is the free-space wavelength at a resonance frequency of the helix and $\lambda_{\rm HX} \approx 35.3$ cm.

Now, a monopole whose length is $L_{\rm MP} = 14$ cm is added to the helix. Note that this length corresponds to approximately $0.4\lambda_{\rm HX}$. The VSWR of the HX-MP with the change in monopole height $z_{\rm MP}$ is shown in Fig. 2(b) and (c). Fig. 2(b) illustrates the case where the monopole is not inserted to the helix. The spacing between the monopole and helix is 0.2 cm $(= z_{\rm MP} - V_{\rm HX} = 6.65 - 6.45$ cm). It is found that the resonance is observed at $f_{\rm HX}$ and the frequency bandwidth for a VSWR $= 2$ criterion increases to approximately 20%.

Fig. 2(c) shows the VSWR when the monopole is slightly inserted to the helix. Note that an upper portion of 0.5 turn of the helix surrounds the monopole $(z_{\rm MP}/V_{\rm HX} = 0.91)$. It is found that two resonance phenomena appear in the vicinity of $f_{\rm HX}$. Low VSWR's are obtained in the lower resonance frequency f_L region and higher resonance frequency f_H region.

As the monopole height $z_{\rm MP}$ further decreases, the separation of the f_H from the f_L becomes wider. This is shown in Fig. 3 as a function of the relative monopole height $z_{\rm MP}/V_{\rm HX}$. The frequency separation ratio f_H/f_L has a maximum value of 2.14 at $z_{\rm MP}/V_{\rm HX} = 0.30$. In this case, the frequency bandwidth for a VSWR $= 2$ criterion is 12.5% in the lower frequency f_L region and 5.2% in the higher frequency f_H region, as summarized in Table I, where the overall antenna height is also presented (the antenna with $z_{\rm MP}/V_{\rm HX} = \infty$ corresponds to the helix without a monopole). Table I reveals that the frequency bandwidth for a VSWR $= 2$ criterion in the lower frequency f_L region is wider than that in the higher frequency f_H region.

Fig. 4(a) shows the total radiation patterns of the HX-MP at f_L and f_H for $z_{\rm MP}/V_{\rm HX} = 0.30$. The E_θ component is a main component of the radiation field. The E_ϕ component is less than -30 dB below the peak of the E_θ component and is not shown in this figure. Measured results are also presented, showing good agreement with calculated ones.

The total radiation from the HX-MP is decomposed into the radiation from the monopole [Fig. 4(b)] and the radiation from the helix [Fig. 4(c)]. It is found that, the radiation patterns for the monopole at f_L and f_H are different, whereas those for the helix remain almost unchanged. It follows that the total radiation pattern is strongly affected by the radiation from the monopole. This can be interpreted by the current distributions $I = I_r + jI_i$ shown in Fig. 5. It is clear that the current distributions along the monopole are different at f_L and f_H, whereas the current distributions along the helix are almost the same.

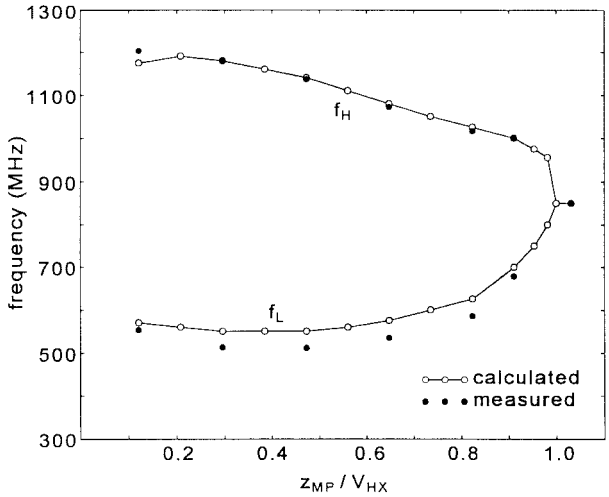

Fig. 3. Higher resonance frequency f_H and lower resonance frequency f_L as a function of relative monopole height $z_{\rm MP}/V_{\rm HX}(= z_{\rm MP}/0.18\lambda_{\rm HX})$. The monopole length $L_{\rm MP}$ is kept constant: $L_{\rm MP} = 14$ cm $\approx 0.4\lambda_{\rm HX}$.

TABLE I
RESONANCE BEHAVIOR AND OVERALL ANTENNA HEIGHT FOR $L_{\rm MP} = 14$ cm $\approx 0.4\lambda_{\rm HX}$

z_{MP}/V_{HX}	VSWR =2 bandwidth (%)		overall height (=L_{MP}+z_{MP})	
	f_L region	f_H region	(cm)	(λ_{HX})
∞	0		6.45	0.18
1.03	20.1		20.65	0.58
0.91	14.9	5.8	19.87	0.56
0.30	12.5	5.2	15.94	0.45
0.12	12.2	3.9	14.77	0.42

The gains at f_L and f_H for a relative monopole height of $z_{\rm MP}/V_{\rm HX} = 0.30$ are approximately 5 and 7 dB, respectively, in the x direction.

C. Effects of Monopole Length $L_{\rm MP}$ on Dual-Frequency Performance

The monopole length $L_{\rm MP}$ is kept constant ($L_{\rm MP} \approx 0.4\lambda_{\rm HX}$) in the previous Section II-B. In this section, the effects of the monopole length $L_{\rm MP}$ on the radiation characteristics are investigated.

Fig. 6 shows the behavior of VSWR relative to 50 Ω for three monopoles. This figure is for monopole lengths $L_{\rm MP} = 0.3\lambda_{\rm HX}, 0.4\lambda_{\rm HX}$ and $0.5\lambda_{\rm HX}$ where the monopole height is kept constant: $z_{\rm MP} = 2.5$ cm $= 0.07\lambda_{\rm HX}$, corresponding to a relative monopole height of $z_{\rm MP}/V_{\rm HX} = 0.39$. It is found that as the monopole length decreases, the lower frequency f_L approaches $f_{\rm HX}$ while the higher frequency f_H goes away from $f_{\rm HX}$. As the monopole length $L_{\rm MP}$ further decreases, the f_H further goes away and the performance of the HX-MP approaches that of the single helix.

The frequency separation ratio f_H/f_L as a function of the relative monopole height $z_{\rm MP}/V_{\rm HX}$ is shown for the three monopoles in Fig. 7. Measured values agree with calculated ones. For the case of a monopole of length $L_{\rm MP} = 0.3\lambda_{\rm HX}$, the frequency separation ratio f_H/f_L has a maximum value of 2.27 at $z_{\rm MP}/V_{\rm HX} = 0.39$.

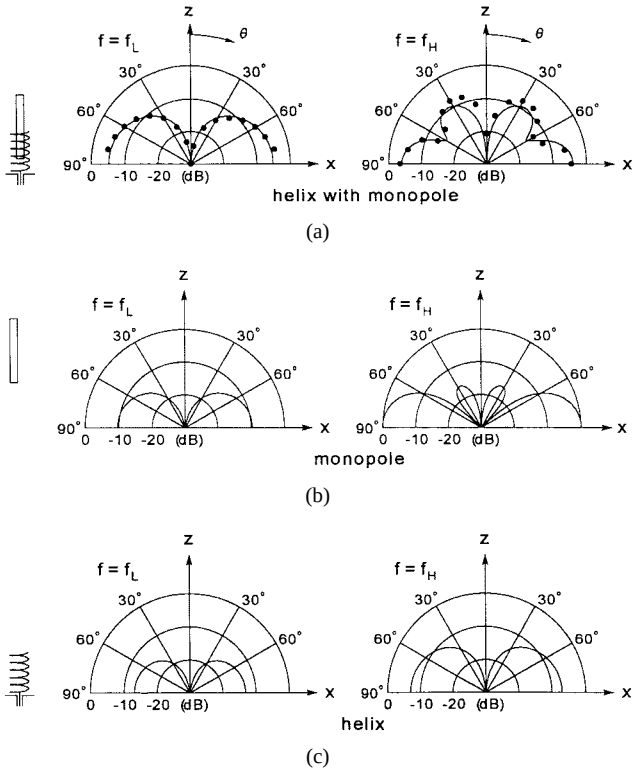

Fig. 4. Radiation patterns at higher resonance frequency f_H and lower resonance frequency f_L. Monopole length is $L_{\rm MP} = 14$ cm $\approx 0.4\lambda_{\rm HX}$ and relative monopole height is $z_{\rm MP}/V_{\rm HX} = z_{\rm MP}/0.18\lambda_{\rm HX} = 0.30$. Calculated E_θ ——— measured E_θ • • •. (a) Total radiation from a helix with a monopole. (b) Radiation from a monopole. (c) Radiation from a helix.

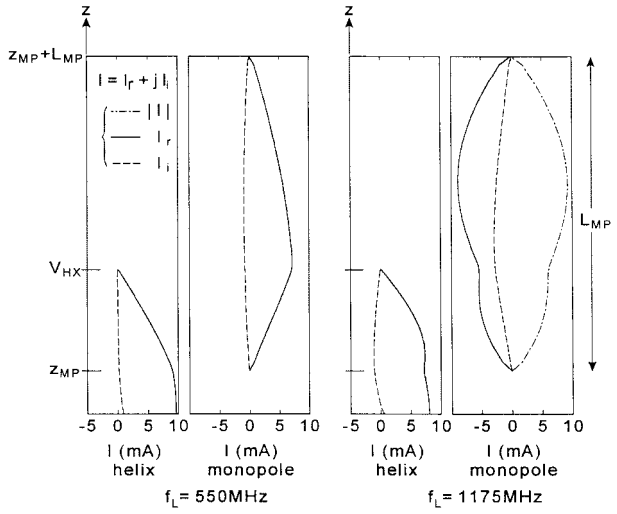

Fig. 5. Current distributions at lower resonance frequency $f_L = 550$ MHz and at higher resonance frequency $f_H = 1175$ MHz. Monopole length is $L_{\rm MP} = 14$ cm $\approx 0.4\lambda_{\rm HX}$ and relative monopole height is $z_{\rm MP}/V_{\rm HX} = z_{\rm MP}/0.18\lambda_{\rm HX} = 0.30$.

III. WIDE-BAND VSWR PERFORMANCE FOR A LOW-PROFILE INVERTED-F ANTENNA WITH PARASITIC ELEMENTS

A monopole parasitic element is useful in widening the frequency bandwidth for VSWR (as well as in generating two resonance frequencies), as observed in Fig. 2(b). In this Section III, two parasitic elements are used for a low-profile antenna to widen the VSWR bandwidth around a center frequency.

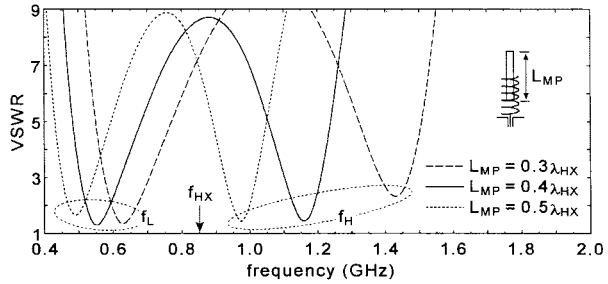

Fig. 6. VSWR's for three values of monopole length $L_{\rm MP}$. The relative monopole height $z_{\rm MP}/V_{\rm HX}$ is kept constant: $z_{\rm MP}/V_{\rm HX} = z_{\rm MP}/0.18\lambda_{\rm HX} = 0.39$.

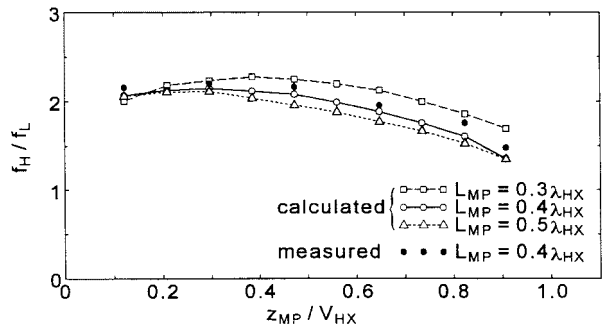

Fig. 7. Frequency separation ratios f_H/f_L as a function of relative monopole height $z_{\rm MP}/V_{\rm HX}(= z_{\rm MP}/0.18\lambda_{\rm HX})$ for three values of monopole height $L_{\rm MP}$.

A. Configuration

Fig. 8(a) shows the configuration and coordinate system of a low-profile IFA with two parasitic elements (IFA-PE) located on a conducting ground plane of infinite extent. The IFA-PE is excited by a coaxial line from point a. The lengths of the horizontal section b–e and vertical section a–b are designated as L_{xo} and h, respectively.

The two parasitic elements are parallel to the IFA with spacing L_y (parasitic element spacing). The arm end of each parasitic element a' is in contact with the ground plane. The horizontal and vertical lengths of the parasitic elements are taken to be the same as those of the IFA. The configuration of the parasitic elements are the same as that of the IFA except for the vertical section c–d.

The section c–d is used for matching the antenna impedance $Z_{\rm ant}$ to the feed line impedance Z_0. The distance from the vertical section a–b to c–d is designated as L_m (matching pin distance). Note that both the IFA and the parasitic elements are made of conducting wires of radius ρ.

The configuration parameters throughout Section III are as follows: $L_{xo} = 4.4$ cm $= 0.1760\lambda_0$, $h = 2.28$ cm $= 0.0912\lambda_0$, $L_y = 5.55$ mm $= 0.0222\lambda_0$, and $\rho = 0.15$ cm $= 0.0060\lambda_0$, where λ_0 is the wavelength at a frequency of $f_0 = 1.2$ GHz. Note that the antenna length $L_{xo} + h(= 6.68$ cm) is longer than $\lambda_0/4(= 6.25$ cm).

B. Wide-Band VSWR Performance

When the matching pin distance is chosen to be $L_m = 8.8$ mm $= 0.0352\lambda_0$, the IFA-PE is matched to a 50-Ω feed line at f_0.

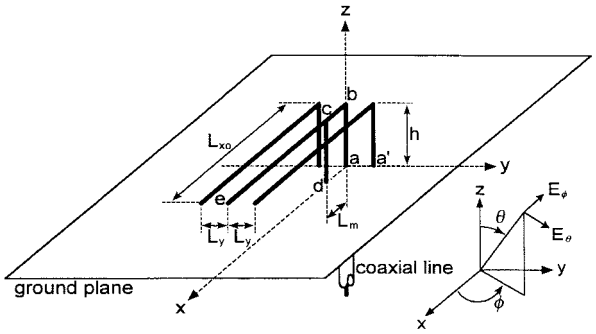

(a)

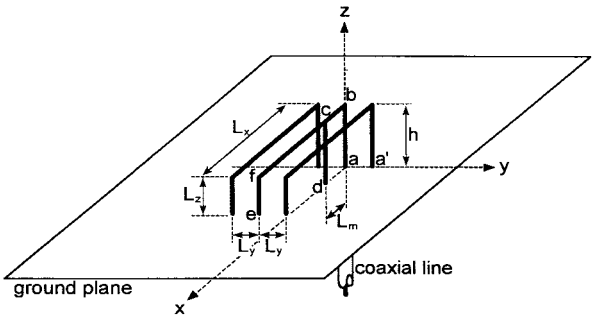

(b)

Fig. 8. Configuration and coordinates. (a) An IFA-PE. (b) A bent IFA-PE.

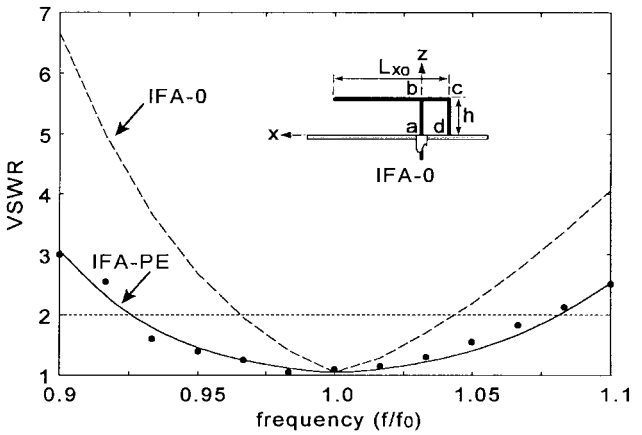

Fig. 9. Frequency response of VSWR. An IFA-PE: calculated ____; measured • • •. An IFA without parasitic elements (IFA-0): calculated - - - -.

Fig. 9 shows the frequency response of the VSWR relative to 50 Ω for the IFA-PE. The frequency bandwidth for a VSWR $= 2$ criterion ($\rm VSWR_2$ bandwidth) is calculated to be approximately 16%. Measured values are also depicted in Fig. 9. The calculated and measured values are in good agreement.

For comparison, the frequency response of the IFA without the parasitic elements (IFA-0) is also illustrated in Fig. 9. The impedance of the IFA-0 is matched to a 50-Ω feed line by locating the section c–d on the $-x$ axis, as shown in the inset of Fig. 9. Note that the impedance matching cannot be obtained by locating the section c–d on the $+x$ axis. The $\rm VSWR_2$ bandwidth is calculated to be 7.9%. Hence, the $\rm VSWR_2$ bandwidth of the IFA-PE is approximately two times as wide as that of the IFA-0. It follows that adding parasitic elements to an IFA contributes to widening the VSWR bandwidth.

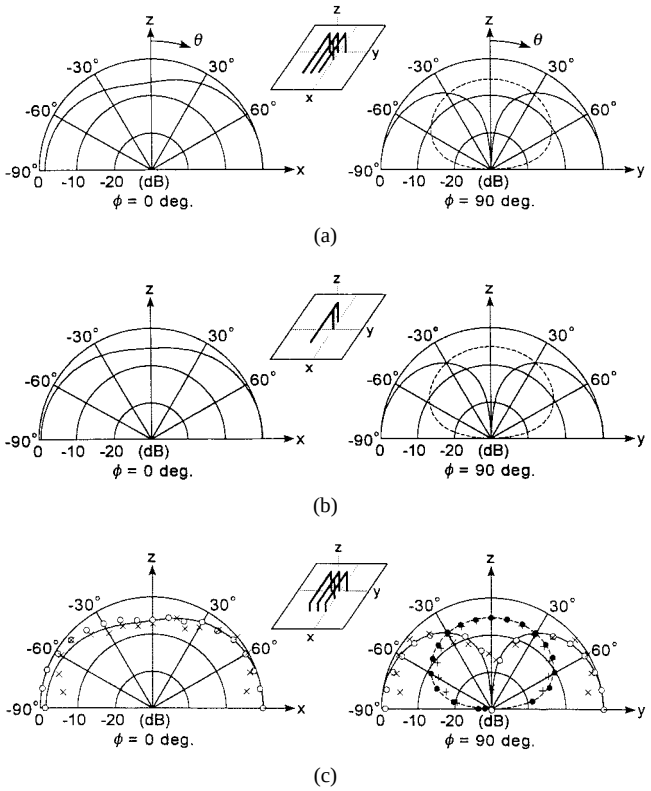

Fig. 10. Radiation patterns. Calculated: E_θ ——; E_ϕ - - - . Measured: E_θ o o o o; E_ϕ • • •. Additional measured results for a finite ground plane of $6\lambda_0 \times 6\lambda_0$ are plotted by crosses ($\times \times \times$) in (c). (a) An IFA-PE. (b) An IFA-0. (c) A bent IFA-PE.

Fig. 10 shows the radiation patterns at f_0, where Fig. 10(a) and (b) are for the IFA-PE and the IFA-0, respectively. It is found that the radiation patterns of (a) and (b) are almost the same, i.e., the parasitic elements do not deteriorate the inherent radiation pattern of the single IFA (IFA-0). Note that the asymmetrical radiation patterns with respect to the z axis in the $\phi = 0°$ plane are due to the asymmetry of antenna configuration with respect to the z axis.

Bending the horizontal sections of the IFA-PE, shown in Fig. 8(b), leads to the downsizing of the antenna. The horizontal section of the IFA is bent at point f, resulting in reduction of the horizontal section length from L_{xo} to $L_{xo} - L_z(\equiv L_x)$, where L_z is the length of the section e–f. Note that the parasitic elements are also bent with the same length L_z. Calculations show that the VSWR_2 bandwidth is approximately 11% for a 20% reduced horizontal length. The radiation pattern for this downsizing configuration is shown in Fig. 10(c). It is seen that the radiation patterns are similar to those of the IFA-0.

The similar radiation patterns Fig. 10(a)–(c) at f_0 result in the almost the same gain. The gains in the x direction are approximately 5 dB for the IFA-PE and the bent IFA-PE, while the gain of the single IFA is 4.4 dB.

IV. Effects of a Finite Ground Plane

So far we have evaluated the radiation characteristics, assuming that the ground plane is of infinite extent. Detailed calculations reveal that the input impedance of the HX-MP is almost constant, provided that the diameter of the ground plane in Fig. 1 is more than 0.5 wavelength. Similar behavior is obtained for the IFA-PE with a square ground plane whose side length is more than 0.5 wavelength in Fig. 8. Hence, a ground plane of 1 m $\times$ 1 m was used to measure the impedance of both the HX-MP and IFA-PE.

An antenna mounted on an infinite ground plane and excited by an unbalanced feed corresponds to an antenna wihout a ground plane excited by a balanced feed (due to image theory). The radiation patterns in Figs. 4 and 10 were measured using the balanced feed instead of the unbalanced feed.

The radiation patterns are affected by ground plane dimensions. The maximum radiation for a finite ground plane is no longer observed in the horizontal plane in Figs. 1 and 8. As an example, the measured radiation pattern for the IFA-PE with a ground plane of $6\lambda_0 \times 6\lambda_0$ is plotted by crosses in Fig. 10(c).

V. Conclusions

Dual-frequency and wide-band VSWR performances are required for wireless communication systems. For these requirements, two antenna systems with parasitic elements are presented.

First, an antenna system composed of a normal-mode helix and a monopole (HX-MP) is analyzed for dual-frequency operation, where the monopole acts as the parasitic element to the helix. The VSWR relative to 50 Ω is evaluated as a function of the monopole height z_{MP}. It is found that the HX-MP resonates in the vicinity of a resonance frequency of the helix f_{HX}.

As the monopole height z_{MP} decreases, the separation of a higher resonance frequency f_H from a lower resonance frequency f_L increases. For the case of a monopole length of $L_{\text{MP}} \approx 0.4\lambda_{\text{HX}}$ and $z_{\text{MP}}/V_{\text{HX}} \approx 0.3$, where V_{HX} is the vertical length of the helix and λ_{HX} is the wavelength at f_{HX}, the frequency bandwidth for a VSWR $= 2$ criterion is 12.5% in the lower frequency f_L region and 5.2% in the higher frequency f_H region, with a frequency separation ratio of $f_H/f_L = 2.14$. The gain is approximately 5 dB at f_L and 7 dB at f_H.

Secondly, a low-profile IFA is investigated to improve the VSWR performance. Adding two parasitic elements (PE) to the IFA increases the frequency bandwidth for the VSWR. The VSWR bandwidth of the IFA-PE is approximately two times as wide as that of the single IFA. It is also found that bending the horizontal section of the IFA-PE elements contributes to the downsizing of the antenna system, not deteriorating the inherent radiation pattern of the single IFA. The frequency bandwidth for a VSWR $= 2$ criterion is 11% for a 20% reduced horizontal length.

References

[1] J. D. Kraus, *Antennas*, 2nd ed. New York: McGraw-Hill, 1988.
[2] R. King, C. W. Harrison, Jr., and D. H. Denton, Jr., "Transmission-line missile antennas," *IEEE Trans. Antennas Propagat.*, vol. 8, pp. 88–90, Jan. 1960.
[3] J. S. Colburn and Y. Rahmat-Samii, "Analysis of a square helix applicable to the personal satellite communication handset," in *IEEE AP-S Symp. Dig.*, Newport Beach, CA, June 1995, pp. 1418–1421.
[4] K. Fujimoto, A. Henderson, K. Hirasawa, and J. R. James, *Small Antennas*. New York: Research Studies Press, 1987, pp. 116–135.

[5] H. Nakano and H. Mimaki, "Normal mode helical antenna with inserted cylindrical conductor," in *Proc. IEICE Fall Conf.*, Tokyo, Japan, Sept. 1992, B-65, p. 65.
[6] ——, "A normal mode helical antenna with a parasitic wire element," in *Proc. IEICE Fall Conf.*, Sendai, Japan, Sept. 1994, B-79, p. 79.
[7] H. Nakano, N. Ikeda, H. Mimaki, and J. Yamauchi, "A normal mode helical antenna (II)," in *Proc. IEICE Gen. Conf.*, Fukuoka, Japan, Mar. 1995, B-155, p. 155.
[8] P. Erätuuli, P. Haapala, and P. Vainikainen, " Dual-frequency wire antennas," *Inst. Electron. Eng. Electron. Lett.*, vol. 32, pp. 1051–1052, June 1996.
[9] E. A. Wolff, *Antenna Analysis*. Boston, MA: Artech House, 1988, ch. 3.
[10] R. J. F. Guertler, "Isotropic transmission-line antenna and its toroid-pattern modification," *IEEE Trans. Antennas Propagat.*, vol. 25, pp. 386–392, May 1977.
[11] T. Tsukiji, "Characteristics of twin rectangular loop antenna and complex loop antennas," *IECE Tech. Rep. Antennas Propagat.*, vol. AP87-43, pp. 63–70, June 1987.
[12] K. Fujimoto and J. R. James, *Mobile Antenna Systems Handbook*. Boston, MA: Artech House, 1994, p. 160.
[13] H. Mishima and T. Taga, "Mobile antenna and duplexer for 800 MHz band mobile telephone system," in *IEEE AP-S Int. Symp. Dig.*, Quebec, Canada, June 1980, pp. 508–511.
[14] H. Nakano, Y. Wu, H. Mimaki, and J. Yamauchi, "An inverted-F antenna with parasitic elements," in *Proc. IEICE Fall Conf.*, Sendai, Japan, Sept. 1994, B-35, p. 35.
[15] ——, "An inverted-F antenna with parasitic elements (II)," in *Proc. IEICE Gen. Conf.*, Fukuoku, Japan, Mar. 1995, B-167, p. 167.
[16] K. Virga and Y. Rahmat-Samii, "An enhanced-bandwidth integrated dual L antenna for mobile communications systems—Design and measurement," in *IEEE AP-S Int. Symp. Dig.*, Newport Beach, CA, June 1995, pp. 1120–1123.
[17] E. Yamashita, Ed., *Analysis Methods for Electromagnetic Wave Problems*. Boston, MA: Artech House, 1995, vol. 2, ch. 3.
[18] R. F. Harrington, *Field Computation by Moment Methods*. New York: Macmillan, 1968.

Hisamatsu Nakano (M'75–SM'87–F'92) was born in Ibaraki, Japan, on April 13, 1945. He received the B.E., M.E., and Dr.E. degrees in electrical engineering from Hosei University, Tokyo, Japan, in 1968, 1970, and 1974, respectively.

Since 1973, he has been a member of the faculty of Hosei University, Tokyo, Japan, where he is now a Professor of electronic informatics. His research topics include numerical methods for antennas, electromagnetic wave scattering problems, and lightwave problems. He was a Visiting Associate Professor at Syracuse University, NY from March through September 1981, where he worked on numerical analysis of electromagnetic coupling between wires and slots. He was also a Visiting Professor at University of Manitoba, Canada from March through September 1986, researching numerical techniques for analysis of microstrip antennas as well as a Visiting Professor at University of California, Los Angeles from September 1986 through March 1987, working on microstrip line-antenna analysis. He has published more than 120 refereed journal papers and 80 international symposium papers on antenna and relevant problems. He is the author of *Helical and Spiral Antennas* (New York: Wiley, 1987). In 1996, he published the chapter "Antenna analysis using integral equations," in *Analysis Methods of Electromagnetic Wave Problems—Volume II* (Norwood, MA: Artech House). He has developed a parabolic antenna using a backfire helical feed for direct reception of the broadcasting satellite TV programs (DBS). He has also developed two types of small indoor flat DBS antennas using novel elements: curled and extremely low-profile helical elements. His other developments include microstrip antennas for global positioning systems (GPS), personal handy telephone antennas, and small dual-polarization Cassegrain antennas for direct reception of communication satellite TV programs.

Dr. Nakano was the recipient of an International Scientific Exchange Award from the Natural Sciences and Engineering Research Council of Canada in 1986. In 1987, he received the Best Paper Award of the Institution of Electrical Engineers Fifth International Conference on Antennas and Propagation. In 1994, he received the IEEE Antennas and Propagation Society Wheeler Award for Best Paper. He is an Associate Editor of *IEEE Antennas and Propagation Magazine*.

Noriaki Ikeda was born in Tokyo, Japan, on June 5, 1971. He received the B.E. and M.E. degrees from Hosei University, Tokyo, Japan, in 1995 and 1997, respectively.

He joined the Matsushita Communication Industrial Co., Ltd., Yokohama in 1997. Mr. Ikeda is a member of the Institute of Electronics, Information, and Communication Engineers of Japan.

Yu-Yuan Wu was born in Taipei, Taiwan, on April 10, 1965. He received the B.E. and M.E. degrees from Hosei University, Tokyo, Japan, in 1993 and 1995, respectively.

He joined Yokowo Manufacturing, Taiwan, in 1997.

Mr. Wu is a member of the Institute of Electronics, Information, and Communication Engineers of Japan.

Ryota Suzuki was born in Kanagawa, Japan, on January 17, 1974. He received the B.E. and M.E. degrees from Hosei University, Tokyo, Japan, in 1996 and 1998, respectively.

He joined the Toshiba Corporation, Tokyo, in 1998.

Mr. Suzuki is a member of the Institute of Electronics, Information, and Communication Engineers of Japan.

Hiroaki Mimaki was born in Yamaguchi, Japan, on December 7, 1952. He received the B.E. degree in electrical engineering from Tokyo Denki University, Tokyo, Japan, in 1976 and the M.E. degree in electrical engineering from Hosei University, Tokyo, Japan, in 1981.

He currently is an Assistant at Hosei University. His research interest is in thin-wire antennas.

Mr. Mimaki is a member of the Institute of Electronics, Information, and Communication Engineers of Japan.

Junji Yamauchi (M'85) was born in Nagoya, Japan, on August 23, 1953. He received the B.E., M.E., and Dr.E. degrees from Hosei University, Tokyo, Japan, in 1976, 1978, and 1982, respectively.

From 1984 to 1988, he served as a Lecturer at the Electrical Engineering Department of Tokyo Metropolitan Technical College, Japan. Since 1988 he has been a Faculty Member of Hosei University, where he is now a Professor of electronic informatics. His research interests include circularly polarized antennas and optical waveguides.

Dr. Yamauchi is a member of the Optical Society of America and the Institute of Electronics, Information, and Communication Engineers of Japan.